NMR Spectroscopy

International Edition: DOI: 10.1002/anie.201510821
German Edition: DOI: 10.1002/ange.201510821

Atomistic Description of Reaction Intermediates for Supported Metathesis Catalysts Enabled by DNP SENS

*Ta-Chung Ong[+], Wei-Chih Liao[+], Victor Mougel, David Gajan, Anne Lesage, Lyndon Emsley, and Christophe Copéret**

Dedicated to Barry K. Sharpless on the occasion of his 75th birthday

Abstract: *Obtaining detailed structural information of reaction intermediates remains a key challenge in heterogeneous catalysis because of the amorphous nature of the support and/or the support interface that prohibits the use of diffraction-based techniques. Combining isotopic labeling and dynamic nuclear polarization (DNP) increases the sensitivity of surface enhanced solid-state NMR spectroscopy (SENS) towards surface species in heterogeneous alkene metathesis catalysts; this in turn allows direct determination of the bond connectivity and measurement of the carbon–carbon bond distance in metallacycles, which are the cycloaddition intermediates in the alkene metathesis catalytic cycle. Furthermore, this approach makes possible the understanding of the slow initiation and deactivation steps in these heterogeneous metathesis catalysts.*

Heterogeneous catalysts are key to efficient processes in the chemical industry. However, they are difficult to improve because of the lack of access to their active-site structures, thus preventing rational approaches to designing better catalysts. Some of the most prominent examples are the Ziegler–Natta and Phillips polymerization catalysts,[1] and the alkene metathesis catalysts based on either supported molybdenum, tungsten, or rhenium oxides.[2] However, little is known about the active-site structures of these industrial heterogeneous catalysts, and it is therefore not surprising that this field is still the focus of many debates and relies on empirical developments.[2,3] One approach to address this problem is surface organometallic chemistry, whose aim is to tailor the structures of active sites by controlled functionalization of surfaces.[4] As modern surface organometallic chemistry provides a means to generate specific active sites, it allows the possibility to determine structure–activity relationships and to implement rational strategies towards better catalyst designs. Even so, the method still faces the difficulty of obtaining structural information with the necessary level of details that is today attainable for the homogeneous analogues. Consequently, active-site structural information is usually acquired by indirect methods, such as comparison with models from molecular analogues.[5] Solution NMR spectroscopy has been particularly powerful in molecular catalysis to directly ascertain the structure and the dynamics of precatalysts or even to detect reaction intermediates.[6] NMR spectroscopy is sensitive to the local environment of the nuclei, and sophisticated multipulse and multidimensional experiments can be tailored to yield information about the electronic structure, the spatial arrangement, the environment, and the connectivity of given nuclei.[7] Today solid-state NMR spectroscopy can also provide a similar level of information for materials,[8] but the method is hindered by the intrinsically poor sensitivity of NMR spectroscopy combined with the fact that only a small fraction of the sample is of interest for surfaces. Therefore, there is a need to develop new approaches to gain access to NMR information of surface sites and reaction intermediates.

In the field of alkene metathesis, DFT studies have revealed that metallacyclobutanes are not only reaction intermediates, but that the trigonal bipyramidal (TBP) isomer is on the reaction pathway, and that the square pyramidal (SP) isomer can be a resting state of the catalyst and/or be involved in deactivation processes (Figure 1).[9] Experimentally, we previously observed that the more-active catalyst **1**, having a less σ-donating ligand ($OtBu_{F9}$),

[*] Dr. T. C. Ong,[+] W.-C. Liao,[+] Dr. V. Mougel, Prof. Dr. C. Copéret
Department of Chemistry and Applied Biosciences, ETH Zürich
Vladimir-Prelog-Weg 1–5, 8093 Zürich (Switzerland)
E-mail: ccoperet@inorg.chem.ethz.ch
Dr. D. Gajan, Dr. A. Lesage
Centre de RMN à Très Hauts Champs, Institut de Sciences Analytiques (CNRS/ENS Lyon/UCB Lyon 1), Université de Lyon
69100 Villeurbanne (France)
Prof. Dr. L. Emsley
Institut des Sciences et Ingénierie Chimiques, École Polytechnique Fédérale de Lausanne (EPFL), 1015 Lausanne (Switzerland)
[+] These authors contributed equally to this work.

Supporting information for this article can be found under http://dx.doi.org/10.1002/anie.201510821.

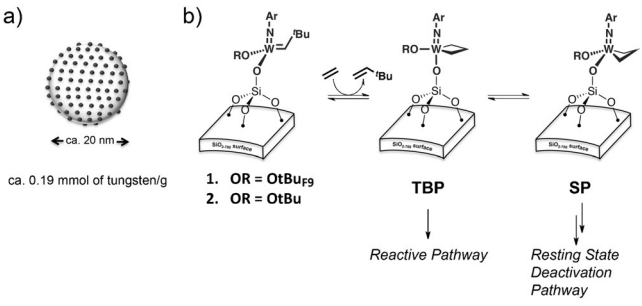

Figure 1. a) Schematic representation of tungsten sites at the surface of SiO_2 nanoparticles. b) Reaction of the tungsten alkylidene sites with ethylene to form the TBP and SP metallacyclobutane intermediates.

primarily generated the TBP isomer and that, in contrast, the less-active catalyst **2**, having a more σ-donating ligand (O*t*Bu), primarily generated the SP isomer.[10] In molecular chemistry the structures of these two isomers were determined by X-ray crystallography[11] and by DFT calculations.[9c] However, diffraction-based techniques are not applicable here because of the amorphous nature of supported catalysts, and the corresponding X-ray absorption techniques only provide an average structure of all surface species, for example, isomers or other species. Recent studies revealed the presence of both TBP and SP intermediates in well-defined supported catalysts using solid-state NMR spectroscopy, albeit at the expense of long experiment time on fully ^{13}C-labeled samples. This low sensitivity limited the studies only to the assignment of surface species by comparison with the known chemical shifts of the corresponding molecular species.[10,12] Obtaining direct structural information, similar to that achieved on a molecular species, for example, C–C connectivity and bond distance measurements, would be a significant step forward in understanding surface site structures, but this step necessitates a major improvement in NMR sensitivity.

In recent years, dynamic nuclear polarization (DNP)[13] has made a major impact on the characterization of surface sites through improving the sensitivity of NMR spectroscopy by up to two orders of magnitude, thereby reducing the need for lengthy signal averaging and improving the detection limit.[14] The technique has the potential to contribute greatly to heterogeneous catalysis research.[15] It has been adapted and applied to the studies of a broad range of materials, including hybrid materials,[14a,b,d] some particularly stable immobilized catalysts,[16] zeolites,[17] and nanoparticles.[14a,b,d,18] However, it has yet to be used to probe the structure of reactive organometallic intermediates with atomic precision. Herein we show that DNP surface-enhanced NMR spectroscopy (DNP SENS), in combination with isotopic labeling, allows us to directly measure structural information of surface reaction intermediates in alkene metathesis catalysts, namely by obtaining C–C connectivities and bond distances of surface-supported metallacyclobutane intermediates (Figure 1). The signal enhancement from DNP also allows observation of the formation of initiation and deactivation products for the catalyst that is slower to initiate and less stable, a process which involves an SP metallacycle intermediate.

Reaction of the catalyst **1**, (≡SiO)W(NAr)(=CH*t*Bu)-(O*t*Bu$_{F9}$),[10] with 10 equivalents of ^{13}C,^{2}H-labeled ethylene liberated 0.8 equivalent of 3,3-dimethyl-1-butene. After contacting the resulting solid with 16 mM of the TEKPol[19] polarizing agent in 1,1,2,2-tetrachloroethane (TCE) by incipient wetness impregnation, the sample was packed into a 3.2 mm sapphire rotor in an argon atmosphere glove box, and cooled to 100 K in the NMR probe. DNP SENS leads to signal enhancements of 23 and 112 for the sample at 600 MHz (14.1 T) and 400 MHz (9.4 T), respectively (Figure 2a). In the latter case, a S/N ratio of about 290 for the major surface species was obtained in only 80 seconds, while 15 hours were previously required to obtain a spectrum with much lower S/N ratio (90) on a 700 MHz (16.4 T) conventional spectrometer

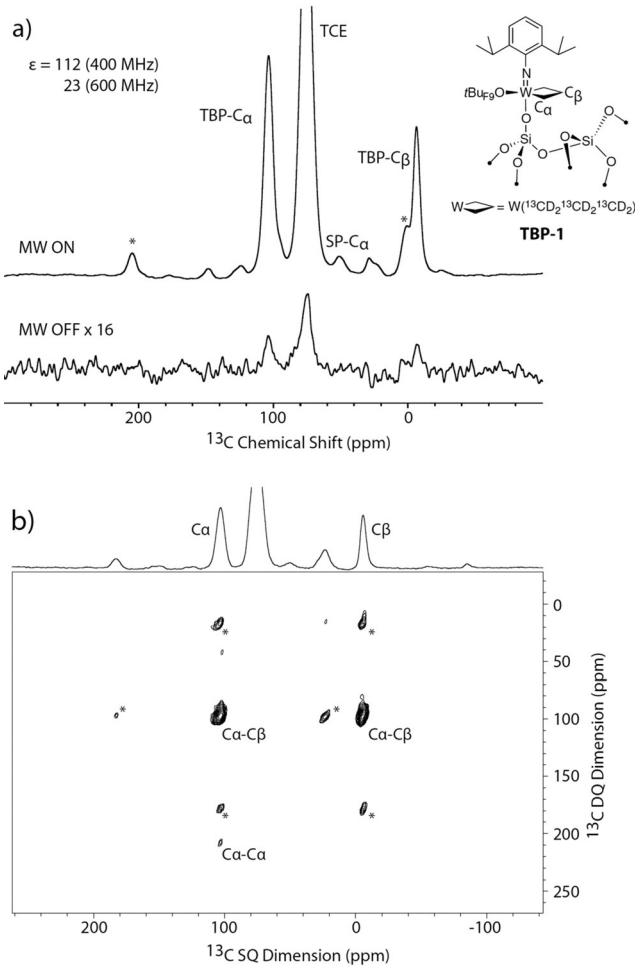

Figure 2. a) ^{13}C DNP SENS CPMAS spectra of ^{13}C,^{2}H-labeled tungsten TBP metallacycle (**TBP-1**). b) 2D DNP SENS refocused INADEQUATE of **TBP-1** showing both the one-bond C_α–C_β and the two-bond C_α–C_α correlations. Both spectra were acquired with a 400 MHz DNP NMR spectrometer. Asterisks indicate spinning sidebands. Experimental parameters are given in the Supporting Information.

at room temperature.[10] The isotropic chemical shifts $\delta_{iso} =$ 102 and −7 ppm are assigned to the C_α and C_β, respectively, of the TBP metallacycle for **1** (**TBP-1**; Figure 2a).[10] The presence of the additional peak at $\delta = 50$ ppm is consistent with the C_α resonance of the associated SP metallacycle **SP-1** as a minor surface species.[10]

A DNP-enhanced two-dimensional (2D) refocused INADEQUATE[20] spectrum (Figure 2b) was recorded to corroborate the assignments. Since the INADEQUATE experiment (sequence shown in Figure S1 in the Supporting Information) is a *J*-based correlation experiment, connectivity through a chemical bond is required to excite double quantum (DQ) coherences. We were able to clearly observe the one-bond C_α–C_β correlation, as well as to detect the weaker two-bond C_α–C_α correlation. We also recorded a 2D POSTC7[21] experiment (sequence shown in Figure S2), which is a homonuclear dipolar recoupling sequence. As with the case of the refocused INADEQUATE spectrum, the C_α–C_β correlation of the TBP metallacycle was clearly observed, while the C_α–C_α correlation was absent (Figure S5). This

absence is most likely due to the effect of dipolar truncation,[22] where the recoupling of the small C_α–C_α dipolar coupling is attenuated in the presence of the stronger C_α–C_β interaction. The presence of only the C_α–C_β dipolar correlation allows the distance between the two nuclei to be measured quantitatively by a series of 1D POSTC7 experiments with different mixing times.[23] Here the DQ efficiency was measured as a function of τ_{ex} by two different methods, that is, the symmetric procedure and the constant-time procedure.[23a,c] The resulting DQ efficiency curves (Figure S8) were simulated using SIMPSON[24] to calculate the C_α–C_β distance, which was found to be (1.54 ± 0.11) Å and is in close agreement with the calculated C_α–C_β distance in the DFT optimized structure (1.59 Å) shown in Figure S3.

By acquiring a CPMAS spectrum at a relatively slow MAS frequency (5.8 kHz), we were able to identify the spinning sidebands associated with the C_α and C_β resonances and measure the chemical shift anisotropy (CSA) parameters for the **TBP-1** (Figure S4a). Deconvolution of the spectrum (Figure S4b–d) allowed us to extract the CSA parameters of each carbon atom (Table 1). The results compare well with those obtained from room-temperature MAS NMR data for both C_α and C_β, and with DFT calculated CSA parameters corrected for spin-orbit coupling in the isotropic shift (δ_{iso}) and span (Ω), which are summarized in Table 1.

Table 1: Experimental and calculated ^{13}C CSA parameters of the TBP metallacycle.[a]

	Conditions	δ_{iso} [ppm]	Ω [ppm]	κ
C_α	100 K DNP	102.1 ± 6.7 (102.7)	180.9 ± 9.5 (194.5)	-0.99 ± 0.17 (-0.69)
C_β	100 K DNP	-7.0 ± 4.2 (-4.5)	101.2 ± 6.0 (81.7)	0.82 ± 0.18 (-0.03)
C_α	RT	102.9 ± 4.6	185.4 ± 6.5	-1.00 ± 0.11
C_β	RT	-2.8 ± 1.6	126.8 ± 2.3	0.82 ± 0.06

[a] DFT calculated values are given within parentheses. The functional/basis set used was B3LYP/TZP corrected for spin-orbit coupling (details are given in the Supporting Information).

Turning to **2**, (≡SiO)W(NAr)(=CH*t*Bu)(O*t*Bu), treatment with ^{13}C,^{2}H-labeled ethylene leads only to 0.2 equivalents of 3,3-dimethyl-2-butene (the cross-metathesis product) under the same reaction conditions, thus indicating slow initiation. Recording DNP SENS under the same conditions (addition of 16 mM TEKPol[19] polarizing agent in TCE) shows an overall signal enhancement of only 70 on the 400 MHz spectrometer (Figure S6), and is possibly due to the presence of the three methyl groups in the O*t*Bu ligand.[14d,25] The two main peaks in the ^{13}C CPMAS spectrum (shown on the top of Figure 3a) can be tentatively assigned to C_α and C_β, respectively, of an SP metallacycle based on comparison with similar molecular species. The 2D refocused INADEQUATE spectrum confirms this hypothesis with a main correlation observed at $\delta = 42$ and 20 ppm in the single-quantum dimension, and therefore the assignment of these peaks to C_α and C_β, respectively, of an SP metallacycle. However, the 2D spectrum also reveals unexpected features, in particular the presence of correlations between two carbon atoms, $\delta =$ 47 and 31 ppm, which appears consistent with an SP metallacycle connected to a tertiary butyl group (Figure 3a).[11b]

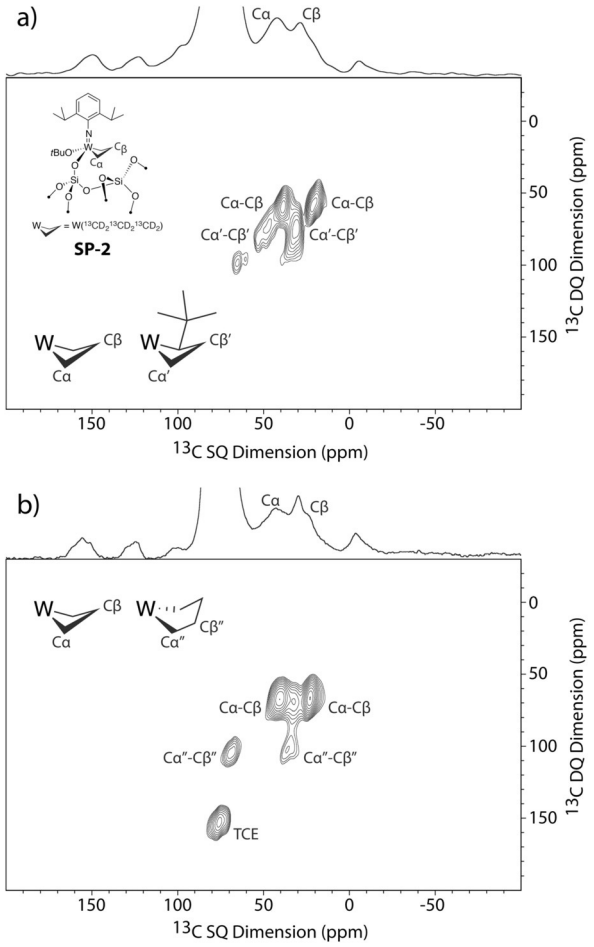

Figure 3. 2D DNP SENS refocused INADEQUATE of: a) **SP-2** obtained by reacting **2** with 10 equiv of labelled ethylene, thus resulting in the presence of both **SP-2** and a tertiary butyl substituted minor species, and b) **SP-2** obtained by exposing **2** to a large excess of ethylene, thus yielding **SP-2** and possibly metallacyclopentane.

We reasoned that the observation of this intermediate metallacycle was probably due to the slow initiation of the metathesis process (Scheme 1). To favor the formation of the parent metallacyclobutane, we thus first exposed **2** to a large excess of ethylene (800 equivalents) for 12 hours and then to 10 equivalents of ^{13}C,^{2}H-labeled ethylene. The 1D ^{13}C NMR spectrum of the material thus formed presents the same overall features as the previous one, with two main peaks at $\delta = 42$ and 20 ppm, which can be assigned to C_α and C_β, respectively, of the SP metallacycle (Figure 3b). However, the 2D INADEQUATE spectrum no longer contains the previously observed correlations associated with the *t*Bu-substituted metallacycle. This data thus confirms the full reaction of the neopentylidene moiety and the formation of the parent

Scheme 1. Initiation mechanism and formation of SP metallacyclobutane and metallacyclopentane from the tungsten neopentylidene.

metallacyclobutane. However, another set of correlations appears at $\delta = 69$ and 36 ppm (marked as C_α'' and C_β'' in Figure 3b), and they are tentatively assigned to a metallacyclopentane moiety formed by a secondary reaction resulting from the presence of a large excess of ethylene.[26] To confirm this hypothesis, Br_2 was introduced into a suspension of this sample in C_6D_6 (see the Supporting Information). ^{13}C NMR data (Figure S10) and GC-MS (Figure S11) analysis of the product solution revealed the presence of 1,4-dibromobutane as a minor product. This observation is consistent with the presence of the proposed metallacyclopentane complex as a minor surface species. The 2D POSTC7 spectra of this material show that the correlation for C_α is inhomogeneously broadened (Figure S7), thus indicating the existence of a distribution of C_α sites. This distribution of sites is not found for the corresponding TBP isomer, likely because the metallacycle lies far from the surface in that geometry, that is, the N-W-OSi angle and the Si–C_α distance are 175° and 4.0–4.1 Å, respectively, for each C_α according to DFT calculations (Figure S3 and associated coordinate file). In contrast, the SP isomer displays an N-W-OSi angle close to 112° and a Si–C_α distance as close as 3.5 Å, thus bringing the metallacycle closer to the surface such that it experiences more the effects of the local environment of the amorphous silica support.

In addition, the 2D POSTC7 spectra reveal the presence of an additional species that is consistent with a TBP metallacycle (Figure S7), but it is not observed in the INADEQUATE experiment (Figure 3b). This observation is most likely due to the lower concentration as well as the relatively small C_α–C_β J coupling (13 Hz)[11b,c,27] of the TBP metallacycle. Although complex, this result allows a more detailed understanding of the initiation and deactivation of **2**. It further highlights the benefit of acquiring complementary 2D NMR spectra, as they reveal molecular features that could not be foreseen from 1D CPMAS spectra on 100% labeled compound. Finally, we further characterized **SP-2** by simulating the POSTC7 DQ curves (Figure S9), which yielded a C_α–C_β distance of (1.49 ± 0.12) Å. While this shorter C_α–C_β distance for the SP metallacycle is consistent with the DFT calculated bond distance and with what is expected for this intermediate,[9c] the precision of the measurement does not allow a clear distinction between the two isomers at the current stage.

In conclusion, we characterized the TBP and SP metallacycle intermediates of tungsten heterogeneous metathesis catalysts by DNP SENS with details at an unprecedented level using a combination of 1D and 2D NMR techniques. This approach allows observation of the surface species at the atomic level, including direct determination of C–C connectivities and bond distances in metathesis reaction intermediates, and monitoring of the initiation and deactivation mechanisms of surface sites in heterogeneous catalysts.

Acknowledgements

We acknowledge the SNF for the 600 MHz DNP spectrometer (206021_150710) and funding for WCL (200020_149704). ERC Advanced Grant No. 320860 is acknowledged for funding support. Dr. René Verel, Prof. Dr. Aaron Rossini, Maxence Valla, and Dr. Daniel Silverio are acknowledged for many useful discussions. Dr. Aleix Comas-Vives and Dr. Francisco Núñez-Zarur are acknowledged for discussions regarding DFT calculations. Dr. Olivier Ouari and Prof. Dr. Paul Tordo are acknowledged for providing the TEKPol biradical. Lénaic Leroux is acknowledged for technical support at C-RMN.

Keywords: DFT calculation · dynamic nuclear polarization · metathesis · solid-state NMR · surface chemistry

How to cite: *Angew. Chem. Int. Ed.* **2016**, *55*, 4743–4747
Angew. Chem. **2016**, *128*, 4821–4825

[1] a) P. Cossee, *J. Catal.* **1964**, *3*, 80–88; b) K. Soga, T. Shiono, *Prog. Polym. Sci.* **1997**, *22*, 1503–1546; c) M. P. McDaniel, *Adv. Catal.* **2010**, *53*, 123–606.
[2] S. Lwin, I. E. Wachs, *ACS Catal.* **2014**, *4*, 2505–2520.
[3] a) B. M. Weckhuysen, I. E. Wachs, R. A. Schoonheydt, *Chem. Rev.* **1996**, *96*, 3327–3349; b) J. J. H. B. Sattler, J. Ruiz-Martinez, E. Santillan-Jimenez, B. M. Weckhuysen, *Chem. Rev.* **2014**, *114*, 10613–10653.
[4] a) C. Copéret, M. Chabanas, R. Petroff Saint-Arroman, J. M. Basset, *Angew. Chem. Int. Ed.* **2003**, *42*, 156–181; *Angew. Chem.* **2003**, *115*, 164–191; b) H. Tada, T. Kiyonaga, S. Naya, *Chem. Soc. Rev.* **2009**, *38*, 1849–1858; c) J. M. Basset, R. Ugo in *Modern Surface Organometallic Chemistry*, Wiley-VCH, Weinheim, **2009**, pp. 1–21; d) S. L. Wegener, T. J. Marks, P. C. Stair, *Acc. Chem. Res.* **2012**, *45*, 206–214; e) M. M. Stalzer, M. Delferro, T. J. Marks, *Catal. Lett.* **2015**, *145*, 3–14; f) C. Copéret, A. Comas-Vives, M. P. Conley, D. P. Estes, A. Fedorov, V. Mougel, H. Nagae, F. Nunez-Zarur, P. A. Zhizhko. *Chem. Rev.* **2016**, *116*, 323–421.
[5] H. P. Jia, E. A. Quadrelli, *Chem. Soc. Rev.* **2014**, *43*, 547–564.
[6] M. D. Christianson, C. R. Landis, *Concept Magn. Reson. A* **2007**, *30A*, 165–183.
[7] P. S. Pregosin, *NMR in organometallic chemistry*, Wiley-VCH, Weinheim, **2012**.
[8] a) K. J. D. MacKenzie, M. E. Smith, *Multinuclear solid-state NMR of inorganic materials*, 1st ed., Pergamon, Oxford, **2002**; b) F. Blanc, C. Copéret, A. Lesage, L. Emsley, *Chem. Soc. Rev.* **2008**, *37*, 518–526.
[9] a) X. Solans-Monfort, E. Clot, C. Copéret, O. Eisenstein, *J. Am. Chem. Soc.* **2005**, *127*, 14015–14025; b) A. Poater, X. Solans-Monfort, E. Clot, C. Copéret, O. Eisenstein, *J. Am. Chem. Soc.* **2007**, *129*, 8207–8216; c) X. Solans-Monfort, C. Copéret, O. Eisenstein, *Organometallics* **2015**, *34*, 1668–1680.
[10] V. Mougel, C. Copéret, *Chem. Sci.* **2014**, *5*, 2475–2481.
[11] a) R. R. Schrock, R. T. Depue, J. Feldman, C. J. Schaverien, J. C. Dewan, A. H. Liu, *J. Am. Chem. Soc.* **1988**, *110*, 1423–1435; b) J. Feldman, W. M. Davis, R. R. Schrock, *Organometallics* **1989**, *8*, 2266–2268; c) J. Feldman, W. M. Davis, J. K. Thomas, R. R. Schrock, *Organometallics* **1990**, *9*, 2535–2548.
[12] a) F. Blanc, R. Berthoud, C. Copéret, A. Lesage, L. Emsley, R. Singh, T. Kreickmann, R. R. Schrock, *Proc. Natl. Acad. Sci. USA* **2008**, *105*, 12123–12127; b) M. P. Conley, W. P. Forrest, V. Mougel, C. Copéret, R. R. Schrock, *Angew. Chem. Int. Ed.* **2014**, *53*, 14221–14224; *Angew. Chem.* **2014**, *126*, 14445–14448.
[13] a) L. R. Becerra, G. J. Gerfen, B. F. Bellew, J. A. Bryant, D. A. Hall, S. J. Inati, R. T. Weber, S. Un, T. F. Prisner, A. E. Mcdermott, et al., *J. Magn. Reson. Ser. A* **1995**, *117*, 28–40; b) T. Maly, G. T. Debelouchina, V. S. Bajaj, K. N. Hu, C. G. Joo, M. L. Mak-Jurkauskas, J. R. Sirigiri, P. C. A. van der Wel, J. Herzfeld, R. J. Temkin, et al., *J. Chem. Phys.* **2008**, *128*, 052211.

[14] a) A. Lesage, M. Lelli, D. Gajan, M. A. Caporini, V. Vitzthum, P. Mieville, J. Alauzun, A. Roussey, C. Thieuleux, A. Mehdi, et al., *J. Am. Chem. Soc.* **2010**, *132*, 15459 – 15461; b) D. Lee, H. Takahashi, A. S. L. Thankamony, J. P. Dacquin, M. Bardet, O. Lafon, G. De Paepe, *J. Am. Chem. Soc.* **2012**, *134*, 18491 – 18494; c) A. J. Rossini, A. Zagdoun, M. Lelli, A. Lesage, C. Copéret, L. Emsley, *Acc. Chem. Res.* **2013**, *46*, 1942 – 1951; d) A. Zagdoun, A. J. Rossini, M. P. Conley, W. R. Gruning, M. Schwarzwalder, M. Lelli, W. T. Franks, H. Oschkinat, C. Copéret, L. Emsley, et al., *Angew. Chem. Int. Ed.* **2013**, *52*, 1222 – 1225; *Angew. Chem.* **2013**, *125*, 1260 – 1263.

[15] T. Kobayashi, F. A. Perras, I. I. Slowing, A. D. Sadow, M. Pruski, *ACS Catal.* **2015**, *5*, 7055 – 7062.

[16] a) M. P. Conley, R. M. Drost, M. Baffert, D. Gajan, C. Elsevier, W. T. Franks, H. Oschkinat, L. Veyre, A. Zagdoun, A. Rossini, et al., *Chem. Eur. J.* **2013**, *19*, 12234 – 12238; b) T. Gutmann, J. Q. Liu, N. Rothermel, Y. P. Xu, E. Jaumann, M. Werner, H. Breitzke, S. T. Sigurdsson, G. Buntkowsky, *Chem. Eur. J.* **2015**, *21*, 3798 – 3805.

[17] a) W. R. Gunther, V. K. Michaelis, M. A. Caporini, R. G. Griffin, Y. Roman-Leshkov, *J. Am. Chem. Soc.* **2014**, *136*, 6219 – 6222; b) P. Wolf, M. Valla, A. J. Rossini, A. Comas-Vives, F. Nunez-Zarur, B. Malaman, A. Lesage, L. Emsley, C. Copéret, I. Hermans, *Angew. Chem. Int. Ed.* **2014**, *53*, 10179 – 10183; *Angew. Chem.* **2014**, *126*, 10343 – 10347.

[18] a) M. Lelli, D. Gajan, A. Lesage, M. A. Caporini, V. Vitzthum, P. Mieville, F. Héroguel, F. Rascon, A. Roussey, C. Thieuleux, et al., *J. Am. Chem. Soc.* **2011**, *133*, 2104 – 2107; b) V. Vitzthum, P. Mieville, D. Carnevale, M. A. Caporini, D. Gajan, C. Copéret, M. Lelli, A. Zagdoun, A. J. Rossini, A. Lesage, et al., *Chem. Commun.* **2012**, *48*, 1988 – 1990; c) O. Lafon, A. S. L. Thankamony, M. Rosay, F. Aussenac, X. Y. Lu, J. Trebosc, V. Bout-Roumazeilles, H. Vezine, J. P. Amoureux, *Chem. Commun.* **2013**, *49*, 2864 – 2866; d) U. Akbey, B. Altin, A. Linden, S. Ozcelik, M. Gradzielski, H. Oschkinat, *Phys. Chem. Chem. Phys.* **2013**, *15*, 20706 – 20716; e) D. Lee, G. Monin, N. T. Duong, I. Z. Lopez, M. Bardet, V. Mareau, L. Gonon, G. De Paepe, *J. Am. Chem. Soc.* **2014**, *136*, 13781 – 13788; f) L. Protesescu, A. J. Rossini, D. Kriegner, M. Valla, A. de Kergommeaux, M. Walter, K. V. Kravchyk, M. Nachtegaal, J. Stangl, B. Malaman, et al., *ACS Nano* **2014**, *8*, 2639 – 2648; g) L. Piveteau, T.-C. Ong, A. J. Rossini, L. Emsley, C. Copéret, M. V. Kovalenko, *J. Am. Chem. Soc.* **2015**, *137*, 13964 – 13971.

[19] A. Zagdoun, G. Casano, O. Ouari, M. Schwarzwalder, A. J. Rossini, F. Aussenac, M. Yulikov, G. Jeschke, C. Copéret, A. Lesage, et al., *J. Am. Chem. Soc.* **2013**, *135*, 12790 – 12797.

[20] A. Lesage, M. Bardet, L. Emsley, *J. Am. Chem. Soc.* **1999**, *121*, 10987 – 10993.

[21] M. Hohwy, H. J. Jakobsen, M. Eden, M. H. Levitt, N. C. Nielsen, *J. Chem. Phys.* **1998**, *108*, 2686 – 2694.

[22] a) P. R. Costa, Massachusetts Institute of Technology (Cambridge, MA), **1996**; b) M. J. Bayro, M. Huber, R. Ramachandran, T. C. Davenport, B. H. Meier, M. Ernst, R. G. Griffin, *J. Chem. Phys.* **2009**, *130*, 114506; c) G. De Paëpe, *Annu. Rev. Phys. Chem.* **2012**, *63*, 661 – 684.

[23] a) M. Carravetta, M. Eden, O. G. Johannessen, H. Luthman, P. J. E. Verdegem, J. Lugtenburg, A. Sebald, M. H. Levitt, *J. Am. Chem. Soc.* **2001**, *123*, 10628 – 10638; b) J. Schmedt auf der Günne, *J. Magn. Reson.* **2003**, *165*, 18 – 32; c) S. Olejniczak, P. Napora, J. Gajda, W. Ciesielski, M. J. Potrzebowski, *Solid State Nucl. Magn. Reson.* **2006**, *30*, 141 – 149.

[24] M. Bak, J. T. Rasmussen, N. C. Nielsen, *J. Magn. Reson.* **2000**, *147*, 296 – 330.

[25] M. Rosay, A. C. Zeri, N. S. Astrof, S. J. Opella, J. Herzfeld, R. G. Griffin, *J. Am. Chem. Soc.* **2001**, *123*, 1010 – 1011.

[26] a) S. Y. S. Wang, D. D. VanderLende, K. A. Abboud, J. M. Boncella, *Organometallics* **1998**, *17*, 2628 – 2635; b) W. C. P. Tsang, K. C. Hultzsch, J. B. Alexander, P. J. Bonitatebus, R. R. Schrock, A. H. Hoveyda, *J. Am. Chem. Soc.* **2003**, *125*, 2652 – 2666; c) A. M. Leduc, A. Salameh, D. Soulivong, M. Chabanas, J. M. Basset, C. Copéret, X. Solans-Monfort, E. Clot, O. Eisenstein, V. P. W. Bohm, et al., *J. Am. Chem. Soc.* **2008**, *130*, 6288 – 6297; d) X. Solans-Monfort, C. Copéret, O. Eisenstein, *J. Am. Chem. Soc.* **2010**, *132*, 7750 – 7757.

[27] A. J. Jiang, J. H. Simpson, P. Muller, R. R. Schrock, *J. Am. Chem. Soc.* **2009**, *131*, 7770 – 7780.

Received: November 23, 2015
Revised: January 29, 2016
Published online: March 8, 2016

